Mathematical Biosciences and Engineering

http://www.aimspress.com/journal/MBE

MBE, 19(5): 4506–4525.
DOI: 10.3934/mbe.2022208
Received: 27 November 2021
Revised: 22 February 2022
Accepted: 22 February 2022
Published: 04 March 2022

Research article

Inter-muscular coherence and functional coordination in the human upper extremity after stroke

Hongming Liu[1,2], Yunyuan Gao[2,3,*], Wei Huang[2], Rihui Li[4], Michael Houston[4], Julia S. Benoit[5], Jinsook Roh[4] and Yingchun Zhang[4]

[1] Zhuoyue Honors College, Hangzhou Dianzi University, Hangzhou 310018, China
[2] College of Automation, Hangzhou Dianzi University, Hangzhou 310018, China
[3] Key labortory of Brain Machine Collaborative Intelligence of Zhejiang Province, Hangzhou 311247, China
[4] Department of Biomedical Engineering, University of Houston, Houston 75835, United States
[5] Texas Institute for Measurement Evaluation and Statistics, University of Houston, Houston 75835, United States

* **Correspondence:** Email: gyy@hdu.edu.cn.

Abstract: Muscle coordination and motor function of stroke patients are weakened by stroke-related motor impairments. Our earlier studies have determined alterations in inter-muscular coordination patterns (muscle synergies). However, the functional connectivity of these synergistically paired or unpaired muscles is still unclear in stroke patients. The goal of this study is to quantify the alterations of inter-muscular coherence (IMC) among upper extremity muscles that have been shown to be synergistically or non-synergistically activated in stroke survivors. In a three-dimensional isometric force matching task, surface EMG signals are collected from 6 age-matched, neurologically intact healthy subjects and 10 stroke patients, while the target force space is divided into 8 subspaces. According to the results of muscle synergy identification with non-negative matrix factorization algorithm, muscle pairs are classified as synergistic and non-synergistic. In both control and stroke groups, IMC is then calculated for all available muscle pairs. The results show that synergistic muscle pairs have higher coherence in both groups. Furthermore, anterior and middle deltoids, identified as synergistic muscles in both groups, exhibited significantly weaker IMC at alpha band in stroke patients. The anterior and posterior deltoids, identified as synergistic muscles only in stroke patients, revealed significantly higher IMC in stroke group at low gamma band. On the contrary, anterior deltoid and pectoralis major, identified as synergistic muscles in control group only, revealed significantly higher IMC in control group in alpha band. The results of muscle synergy and IMC analyses provide congruent and complementary information for investigating the mechanism that underlies post-stroke motor recovery.

Keywords: electromyography; muscle synergy; non-negative matrix factorization; inter-muscular coherence; stroke

1. Introduction

Stroke is the second leading cause of disability among adults worldwide, accounting for 6.55 million deaths in 2019 [1]. Motor impairment caused by stroke may affect the ability of patients to coordinate the regular activation of muscles, and negatively impact the activities of daily living [2]. A number of studies have shown the anomalous coupling between torques at the shoulder and elbow. For instance, Beer et al. reported that the obvious weakness of elbow flexion and extension in paresis depends largely on the direction and magnitude of the abduction/adduction torque generated by the shoulder [3]. Lan et al. found that abnormal shoulder abduction loading could reduce the patients' ability to voluntarily open their hands and control their grip after stroke [4]. In addition, Sukal et al. demonstrated that due to the higher degree of shoulder abduction of the paresis limbs, the abnormal coupling of elbow flexion increased [5]. Another previous study suggested that coordination of elbow extensor and shoulder flexor muscle activation during arm extension is weakened in stroke patients, leading to the poor performance of common motor tasks [6]. These findings provide experimental evidence that investigating the intermuscular interaction might be beneficial to uncover the mechanism underlying the recovery of motor function after stroke.

Considering the redundancy of the muscular skeletal system, lots of studies have assumed that the central nervous system (CNS) simplifies motor control by simultaneously activating multiple muscles as a motor module, also known as muscle synergy, defined as consistent intermuscular coordination patterns that are flexibly activated to produce a variety of movement, instead of individually, to conquer the problem of high degrees of freedom in the musculoskeletal system [7, 8]. In recent years, muscle synergy analysis has been widely applied to uncover how muscles are coordinated during a variety of complex movements. For instance, Roh et al. applied non-negative matrix factorization (NMF) to address whether stroke induces changes in the synergy of human upper limb muscles during isometric muscle strength generation. The results showed that alterations in two shoulder muscle synergies appear prominently in seriously injured stroke survivors as well as in mildly and moderately impaired ones [9, 10]. In their study of the human lower extremity, Clark et al. suggested that composition of muscle synergies remained unchanged after stroke, whereas the ability to independently activate the conserved synergies was affected in stroke during walking [11]. It was also reported that fewer synergies were activated during gaits in individuals with cerebral palsy compared with neurologically unimpaired individuals [12]. Despite the aforementioned findings, one main limitation of muscle synergy analysis is that it can only reflect the spatiotemporal anatomical coordination of multiple muscles and assess the activation status of overall muscle activity [13], yet it fails to uncover the neurophysiological mechanisms underlying the formation of muscle synergies [14].

Coherence analysis is an effective method to evaluate the neural synchronization between muscles or brain regions [15, 16], and it is typically based on the cross-correlation between signals in the frequency domain [17]. Recent studies have shown that inter-muscular coherence (IMC) is able to

characterize the strength of neural synchronization at different frequency bands [18]. Kisiel-Sajewicz et al. reported that stroke patients with poor performance in reaching tasks exhibited weaker intermuscular coupling in a low-frequency range (0–11 Hz) [2]. In addition, Fisher et al. found IMC at beta (15–30 Hz) frequency band can be used as a synchronous index to assess the motor dysfunction of the upper limb of stroke patients [19]. Though IMC is able to characterize the muscular coupling between the activation of two muscles, it fails to consider the inherent synergistic effect in all target muscles, rendering it more difficult to interpret the result of IMC analysis [20]. To address this issue, Farmer et al. proposed the motor binding hypothesis that muscular coupling should be primarily associated with the synergistic property of muscles [21]. In support, recently a few studies have attempted to analyze EMG signals by combining the muscle synergy theory and IMC analysis [14, 20, 22]. Specifically, muscle synergy analysis was used to identify synergistic or non-synergistic muscle pairs, and subsequently, coherence analysis assessed the IMC between these muscle pairs. While these studies have demonstrated promising results by combining the muscle synergy theory and IMC analysis in healthy subjects, it remains unknown how the neural synchronizations of synergistic or non-synergistic muscle pairs are modulated after stroke. Therefore, there is a clear need to investigate the alterations of intermuscular coupling in stroke patients using the combination of muscle synergy and coherence analyses. The goal of this study was to investigate the IMC of synergistic or non-synergistic muscle pairs in stroke patients and healthy participants during a three-dimensional (3-D) isometric force generation task [9]. We hypothesized that the impairment of spatial muscle coordination of stroke patients would be related to variations in the composition of muscle synergy and changes in IMC between synergistic muscles. To test the hypothesis, surface EMG signals from key elbow and shoulder muscles were recorded in a 3-D force matching protocol executed by stroke patients and age-matched, neurologically-intact participants. The EMG signals were then processed using a combination of muscle synergy and IMC analysis strategy for all subjects.

2. Materials and methods

2.1. Participants and data source

The data used in this study were the same to our previous publication [9], which was recorded from the affected arm only of 10 stroke survivors (S1-10, age: 62.3 ± 9.3 years), and both arms of 6 age-matched control subjects (C1-6, age: 63.2 ± 7.6 years). More information for the stroke survivors are summarized in Table 1 [9]. All participants in both groups were right-handed. Subjects in control group had no muscular or orthopedic injuries in their upper limbs and were neurologically healthy. The study was performed according to the Declaration of Helsinki and was approved by the Institutional Review Board of Northwestern University. Informed consent of each subject was obtained before the testing.

2.2. Equipment

3-D forces generated by hand and the position of the hand were recorded by the Multi-Axis Cartesian-based Arm Rehabilitation Machine (MACARM) (Figure 1A). The MACARM is composed of a 8 actuators' cubic array, connected to the central end-effector through a cable (more details please

Table 1. Demographic data and clinical scores for stroke survivors.

Subject	Age /sex	Years since onset	Type of stroke	Fugl-Meyer Assessment score /66	/24	Modified Ashworth score (FL/EX)	Lesion location
S1	55/M	22.6	IS	13	9	1+/1	R, frontolateral region
S2	62/F	7.3	HE	15	9	1+/1	L, middle cerebral artery (MCA)
S3	52/F	25.2	IS	12	10	3/2	R, anterior MCA in posterior frontal lobe
S4	65/M	11.1	IS	23	12	1+/1	L, MCA involving L frontotemporal region and temporal lobe
S5	70/M	18.1	HE	19	12	2/0	R, frontoparietal
S6	81/M	16.6	IS	19	10	4/0	L, parietal
S7	53/F	6.7	HE	19	12	1+/1+	R, basal ganglia and occipital horn involvement
S8	59/F	23.4	HE	20	10	2/1+	unavailable
S9	70/F	21.5	IS	20	10	3/0	L, basal ganglia and centrum semi-ovale
S10	56/M	5.7	IS	19	12	3/0	L, basal ganglia or lateral thalamic infarct

M, male; F, female. IS, ischemic; HE, hemorrhagic. Total scores for entire assessment of Fugl-Meyer scale are 66; Subscores related to shoulder and elbow function inside and outside the synergies are 24 (the pronation/supination components are removed). Modified Ashworth score of elbow (0 means normal function; 4 means severe spasticity). FL, flexion; EX, extension. R, right; L, left.

refer to [23, 24]), described in depth in the previous researches [9, 10]. Subjects grasped the gimbaled handle, mounted on a six-degree-of-freedom (DOF) load cell (Model #45E15A, JR3, Woodland, CA). Forces were sampled at a frequency of 64 Hz and stored on a computer for subsequent analysis.

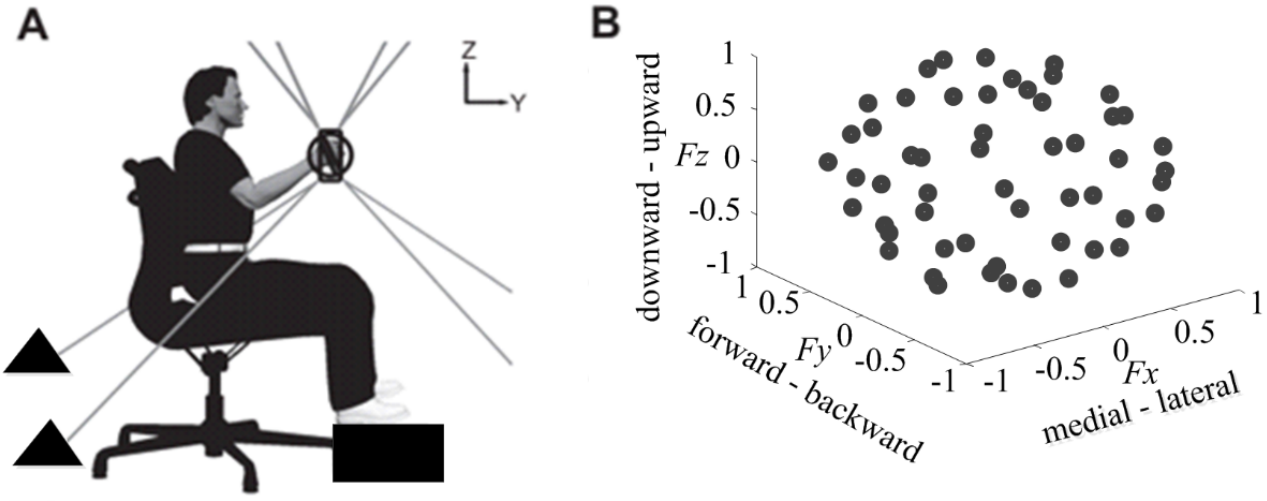

Figure 1. Schematic diagram of the experiment, in which each subject sat down to prepare for the target matching test. A. Side view of the experimental device. The coordinate system for force and position measurements is right-handed (i.e., the x-axis faces the reader) and indicated at the uppper right. Z and Y are the directions of upward-downward and forward and backward, respectively. B. The 54 normalized targets in the 3-D space. Each dot corresponds to the end-point of a target force vector.

2.3. Electromyography

Surface EMGs were recorded from eight key shoulder and elbow muscles. They include brachioradialis (BRD); biceps brachii (BI); triceps brachii, long and lateral heads (TRIlong and TRIlat, respectively); deltoid, anterior, middle and posterior fibers (AD, MD and PD, respectively); and pectoralis major (clavicular fibers, PECTclav). Electrodes were placed according to Hermens et al. (1999) and Delagi and Perotto (1980). EMG signals were sampled at 1,920 Hz, amplified (× 1,000), band-pass filtered (20–450 Hz).

2.4. Protocol

The experimental protocol was as same as the previous study [9]. Subjects sat on an adjustable chair while grabbing the handle of Markham's frame and placing their hands in front of the shoulder on the same side, at 60% of the arm length (Figure 1A). After a brief training, subjects generated voluntary forces in 54 distinct directions (the black dots representing the endpoints of target force vectors; Figure 1B), nearly evenly scattered in 3-D space. The intensity of the force was set to 40% of the utmost sideward force. In this direction, all subjects had the minimum MVCs. In each trial, the target match task was started after the 2-second baseline interval. Healthy subjects and stroke patients were given

9 and 11 seconds respectively to achieve target matching. And the matching speed was determined by the subjects. After the target match was successful, the subject was required to maintain 1 second, followed by the next target match task at a random sequence. Each subject has three chances to try to match each target. In order to prevent the subjects from feeling fatigued, a 10-s inter-trial interval and a 1-min resting interval after 10 trials were provided. Stroke survivors use only the affected limb to complete the protocol.

2.5. NMF-based muscle synergy identification and classification of synergistic and non-synergistic muscle pairs

Prior to the IMC analysis, we applied an NMF algorithm [25] to the EMG datasets collected from eight muscles to extract muscle synergies and their corresponding activation weights. The description of NMF-based muscle synergy extraction was introduced in our previous publication in detail [9]. In brief, baseline voltage drift was removed from EMGs. And EMGs were then corrected and averaged over the target matching interval. Mean baseline EMGs were subtracted from the averaged data. To extract synergy by NMF, the small negative values were set to zero [26,27]. Before extracting synergy, each muscle's EMGs were concatenated across trials related to the aim of the synergy extraction and standardized to unit variance. It ensured that high-variance muscles were not be biased in later synergy extraction from preprocessed EMGs. For each synergy resulting from each extraction, according to their relative contribution to the synergy, the corresponding muscle pairs are selected for subsequent coherence analysis. Specifically, every muscle synergy vector W is normalized so that its value is in the range [0–1]. After normalization, if the contribution of the muscle to the synergistic vector W is greater than 0.25, the muscle is considered to be active within the synergy [9]. Very briefly, the NMF-based muscle synergy analysis is given as:

$$M_{iu} \approx (WC)_{iu} = \sum_{j=1}^{n} W_{ij} C_{ju} = \widetilde{M_{iu}} \tag{2.1}$$

where M_{ij} was a matrix with 8 rows and N columns. It contained N synergies (of unit magnitude, $i = 8$, $j = N$) in every column. C_{ju} was a matrix with N rows and T columns (amount of trials, $\mu = T$) matrix andevery column of it contained a specific trial's synergy activation coefficients. For each arm, M_{iu} was a matrix with 8 rows and T columns. M_{iu} is the original matrix, and $\widetilde{M_{iu}}$ is the data matrix reconstructed by the NMF algorithm. To determine the minimum amount of muscle synergies, we calculated variance accounted for (VAF) measure:

$$VAF = 1 - \frac{RSS}{TSS} = 1 - \frac{\sum \left(M_{iu} - \widetilde{M_{iu}}\right)^2}{\sum M_{iu}^2} \tag{2.2}$$

where RSS is the sum of the squared residuals, TSS is the sum of squared EMG signals. The amount of synergy on which each data set is defined as the minimum amount of synergy required to reach an average global $VAF > 90\%$ while meeting local fit criteria (adding another synergistic increase mean $VAF < 3\%$).

2.6. Coherence analysis

The raw EMG signals were first filtered with a 4th-order Butterworth band-pass filter (5~200 Hz) to extract the valuable information of EMG signals. After filtering, in order to optimize the temporal

imformation of motor unit action potentials, full-wave rectification was performed [28]. In addition, to obtain unit variance, all rectified EMG signals were normalized [29]. To calculate the coherence of muscle pairs, we first divide the target force space into 8 subspaces, A1-A8 defined in Cartesian coordinates ([+Fx, +Fy, +Fz] = [lateral, forward, upward direction]; Area1, [+Fx, +Fy, +Fz]; Area, [+Fx, -Fy, +Fz]; Area3, [-Fx, -Fy, +Fz]; Area4, [-Fx, +Fy, +Fz]; Area5, [+Fx, +Fy, -Fz], Area6, [+Fx, -Fy, -Fz]; Area7, [-Fx, -Fy, -Fz]; and Area8, [-Fx, +Fy, -Fz]). Per each muscle, the EMG data that corresponded to the target forces categorized within the same subspace were concatenated and coherence was calculated per each subspace.

The coherence of any muscle pairs within any subspace was then obtained as:

$$C_{xy}(\lambda)^2 = \frac{\left|f_{xy}(\lambda)\right|^2}{f_{xx}(\lambda)\, f_{yy}(\lambda)} \tag{2.3}$$

where the $f_{xx}(\lambda)$ and $f_{yy}(\lambda)$ are auto-spectrums of the EMG signals of any muscle pair at a given frequency and $f_{xy}(\lambda)$ is the cross-spectrum between them. The fast Fourier transform (FFT) window was set to 0.2 s without overlapping to achieve a frequency resolution of 1.07 Hz. To quantify the significance of the coherence between two muscles, a measure named as confidence level (CL) was introduced [30]:

$$CL = 1 - (1 - \alpha)^{\frac{1}{L-1}} \tag{2.4}$$

where α is the degree of significance ($\alpha = 0.95$) and L is the amount of data segments participating in spectrum estimation. The coherence between two muscles is considered to be significant when the corresponding coherence value is higher than CL, and vice versa.

2.7. Statistical analyses

To assess the coherence strength of the IMC of any muscle pair activated during force generation in both control and patient groups, we introduced the measure of significant coherence area, A, defined as the area above confidence level:

$$A = \sum_{\lambda} \Delta\lambda \left(C_{xy}(\lambda) - CL\right) \tag{2.5}$$

where λ denotes the frequency bin. The larger the value of A, the more significant the coherence in a particular frequency band. Before statistical comparison, the coherence of C_{xy} were normalized by Fisher's -r-to-z transform [$F_z = atanh(r)$] [31].

We first evaluated the difference of IMC between synergistic and non-synergistic muscle pairs in all participants. The significant coherence area values of all muscle pairs per each sub-space of target forces were averaged separately for each subject, resulting in one mean muscular coupling index for each synergistic or non-synergistic muscle pair in a sub-space. A paired t-test was then brought out separately to evaluate the difference of IMC between synergistic and non-synergistic muscles within each subspace for both control and stroke groups. In addition, we also aimed to document how the frequency-specific muscular coupling is altered after stroke by testing the difference of significant coherence area between control and stroke groups for each muscle pair, especially the synergistic muscle pairs. The whole frequency range was first divided into three frequency components, including alpha (α, 8–14 Hz), beta (β, 14–30 Hz) and low gamma (γ, 30–60 Hz). These frequency

bands have previously been determined to be physiologically relevant in neuromuscular control. Then the significant coherence area of each muscle pair was obtained for each frequency component in each sub-space of target forces. The difference between control and patient groups in terms of each muscle pair and each frequency band was tested by two-sample t-tests. What's more, based on the results of traditional scale method and conherence analysis of synergistic muscle pairs of stroke patients, the significant area index of frequency band was selected. Then, the correlation between the multi-band coherence of synergetic muscles and the scores of clinical Fugl-Meyer scale was analyzed by Pearson coefficient. The possibility of synergetic muscle pair coherence as an auxiliary index for the evaluation of motor function in stroke patients was verified. The significance level of all tests was set to 0.05.

3. Results

3.1. EMG coherence analysis among synergistic and non-synergistic muscle pairs

Prior to the IMC analysis, the synergistic and non-synergistic muscle pairs were extracted. Methods and results were shown in our previous publication [9,32]. In brief, the EMG was parsed into four parts, including three force rising stages and one force maintenance stage, namely stages RAMP1, RAMP2, RAMP3 and HOLD. After connecting the data obtained from 54 points in the space, an 8×54 matrix was constructed. Through the NMF of the matrix, the synergistic muscle base matrix of the four stages was obtained, and then the synergistic muscle pairs can be found. In summary, four synergistic muscle pairs, including BRD-BI, TRIlat-TRIlong, AD-MD and MD-PD, were identified from both control and stroke groups. The synergistic muscle pairs, including AD-PECTclav and MD-PECTclav, were identified only in the control group, while the synergistic muscle pair AD-PD was identified only in the stroke group. The rest of the possible muscle pairs were classified as non-synergistic pairs for either control or stroke group. The IMC analysis was then performed on both synergistic and non-synergistic muscle pairs. The details are summarized in Table 2.

In the control group, synergistic muscle pairs revealed higher coherence during the force generation compared to the non-synergistic muscle pairs at each sub-space (Figure 2). In the figure, the horizontal coordinates represent the frequency band and the vertical coordinates represent the coherence of synergetic and non-synergetic muscles. Specifically, the coherence of most synergistic muscle pairs exhibited significantly higher ($p = 0.0103 < 0.05$) coherence than the confidence level (Figure 2A). In addition, two representative non-synergistic muscle pairs identified in the control group, the AD-PD pair and PD-PECTclav pair, were shown as a contrast to the synergistic muscle pairs, wherein coherence of each non-synergistic muscle pair tended to be significantly lower ($p = 0.0146 < 0.05$) than the confidence level (Figure 2B). Though not shown in Figure 2B, similar non-significant coherence was observed at each non-synergistic muscle pairs. It was also found that synergetic and non-synergetic muscles had relatively consistent coherence results in the eight subspaces. And the statistical data show that there was no significant difference in the coherence of the eight subspaces (synergetic muscles, p = 0.952; non-synergetic muscles, p = 0.875). It explained that when the nerve center controled the movement, it controled the movement by controlling the synergetic module. The same motion mechanism did not change the motion control mode in different motion directions.

In the patient group, synergistic muscle pairs also held a higher coherence compared to

Table 2. Summary with the pairs of synergistic and non-synergistic muscle pairs for control and stroke.

	Synergistic muscle pairs		Non-synergistic muscle pairs	
	Together	Single	Together	Single
Stroke	BRD-BI, TRIlat-TRIlong, AD-MD, MD-PD	AD-PD	BRD- TRIlat, BRD-TRIlong, BRD-AD, BRD-MD, BRD-PD, BRD-PECTclav, BI-TRIlat, BI-TRIlong, BI-AD, BI-MD, BI-PD, BI-PECTclav, TRIlat-AD, TRIlat-MD, TRIlat-PD, TRIlat-PECTclav, TRIlong-AD, TRIlong-MD, TRIlong-PD, TRIlong-PECTclav, PD-PECTclav	AD-PECTclav, MD-PECTclav
Control		AD-PECTclav, MD-PECTclav		AD-PD

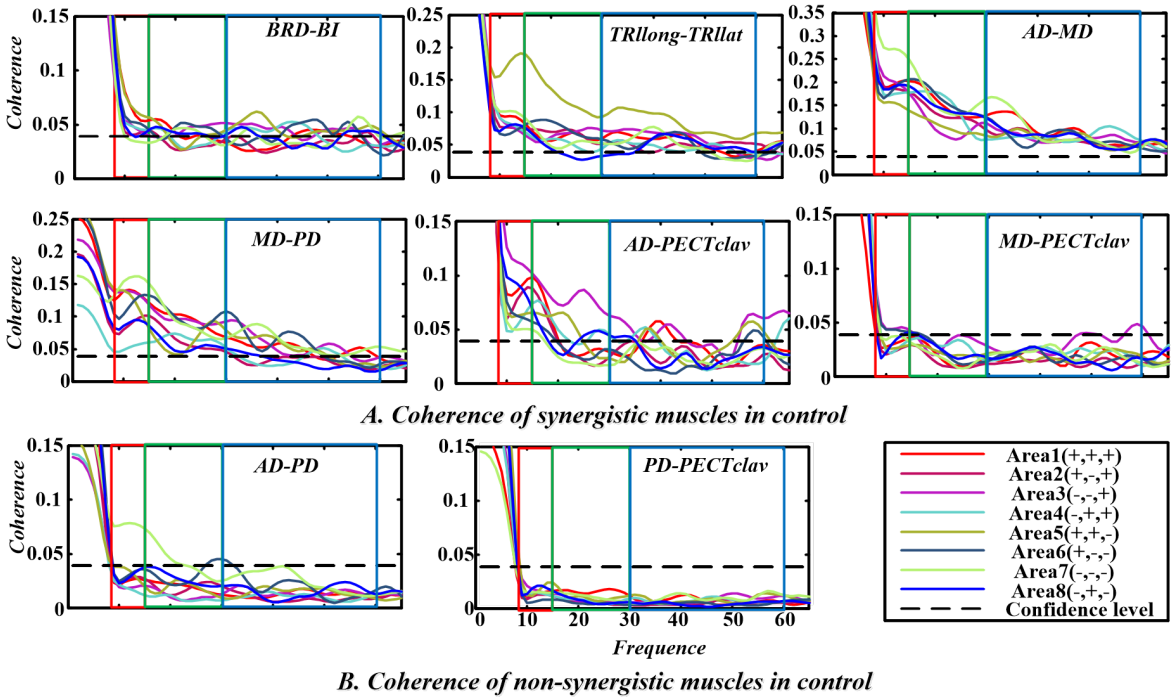

Figure 2. Coherence analysis of synergistic muscles (A) and non-synergistic muscles (B) in the control group at eight subspaces. The rectangular red, green, and blue lines indicated the range of α, β, and low γ bands, respectively. The axis for muscles is not the same.

non-synergistic muscle pairs in most sub-spaces (Figure 3). In the figure, the horizontal coordinates represent the frequency band and the vertical coordinates represent the coherence of synergetic and non-synergetic muscles. The coherence of three representative non-synergistic muscle pairs identified in the stroke group, AD-PECTclav, MD-PECTclav and PD-PECTclav, was shown as a contrast to that of the synergistic muscle pairs in stroke. Similarly, the coherence of synergistic muscle pairs was higher ($p = 0.0174 < 0.05$) than the confidence level (Figure 3A), while coherence of any non-synergistic muscle pair was significantly lower ($p = 0.0243 < 0.05$) than the confidence level (Figure 3B). And it was found that there was no significant difference in the coherence of the eight subspaces (p = 0.628), which was the same as that of the control group.

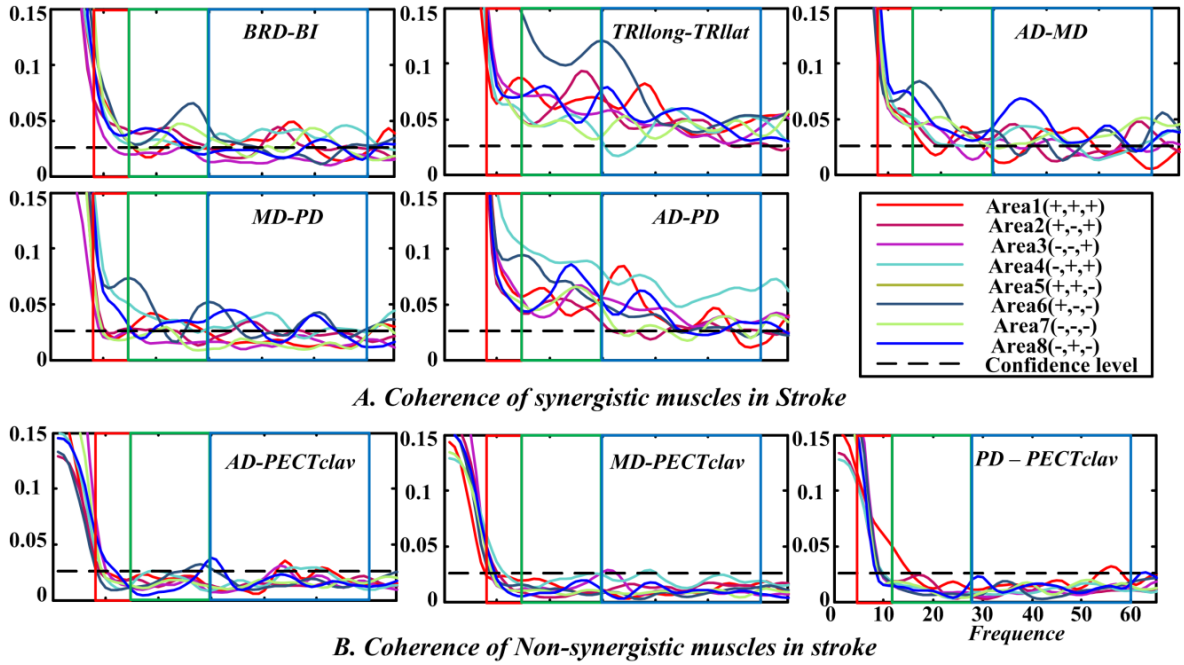

Figure 3. Coherence analysis of synergistic muscles (A) and non-synergistic muscles (B) in stroke patients at eight subspaces.

The statistical analysis of the significant coherence area showed that, for both healthy and stroke groups, respectively, synergistic muscle pairs consistently yielded higher coherence strength during the force generation under isometric conditions compared to the non-synergistic muscle pairs across all sub-spaces ($p < 0.004$). Multiple comparisons for eight simultaneous t-tests were corrected using Bonferroni method ($p_{corrected} = 0.00625$). The details of the statistical analyses are summarized in Table 3. The values presented in Table 3 are averaged over the entire frequencies (8~60 Hz), which is the main frequency content for information in the central nervous system. The result shows that synergistic muscles generally yield higher coherence strength than non-synergistic muscles.

3.2. Comparison of coherence between control and stroke groups

Figure 4 shows the comparison of coherence strength (assessed by significant coherence area) between control and stroke groups with respect to muscle pair and frequency band. Based on our previous work [9], 28 pairs of muscles were divided into four groups, including synergistic muscle

Table 3. Summary of the statistical analysis on significant coherence area of synergistic and non-synergistic nuscle pairs.

	Control			Stroke		
Subspace	Coherence of Synergistic Muscle Pairs	Coherence of Non-synergistic Muscle Pairs	p – value	Coherence of Synergistic Muscle Pairs	Coherence of Non-synergistic Muscle Pairs	p – value
	Mean ± Std	Mean ± Std		Mean ± Std	Mean ± Std	
Area 1	1.290 ± 2.083	−1.123 ± 0.611	<0.001	0.824 ± 0.930	−0.553 ± 0.318	<0.001
Area 2	1.049 ± 1.961	−1.001 ± 0.470	<0.001	0.591 ± 0.608	−0.363 ± 0.439	<0.001
Area 3	1.107 ± 1.450	−1.387 ± 0.770	<0.001	0.985 ± 1.064	−0.072 ± 0.569	0.004
Area 4	0.905 ± 1.825	−1.230 ± 0.499	<0.001	1.587 ± 1.172	−0.090 ± 0.627	<0.001
Area 5	0.829 ± 1.980	−1.356 ± 0.911	<0.001	1.333 ± 0.994	−0.329 ± 0.662	<0.001
Area 6	1.148 ± 1.974	−1.178 ± 0.505	0.001	1.415 ± 1.359	−0.549 ± 0.346	<0.001
Area 7	1.102 ± 2.412	−1.123 ± 0.504	<0.001	1.462 ± 0.752	−0.097 ± 0.349	<0.001
Area 8	0.712 ± 1.860	−1.327 ± 0.547	<0.001	1.581 ± 0.711	−0.009 ± 0.547	<0.001

$p_{corrected}$ = 0.00625 after Bonferroni correction.

pairs in stroke and control groups, synergistic muscle pairs in stroke group only, synergistic muscle pairs in the control group only, and non-synergistic muscle pairs in both groups (Figure 4). Among the synergistic muscle pairs identified in both groups in Figure 4 (colored in yellow), the coherence strength between AD-MD muscles was found to be significantly reduced ($p = 0.011$) in stroke patients compared to the control at α band. Furthermore, the AD-PD muscle pair (Blue), which was identified as synergistic muscles only in the stroke patients, revealed significantly higher ($p = 0.023$) coherence strength at low γ band in stroke patients. On the contrary, AD-PECTclav muscle pair, identified as synergistic muscles in the control group only, yielded significantly higher ($p < 0.01$) coherence strength at α band in the control group (colored in purple). In addition, no significant difference ($p > 0.05$) was found between control and patient groups on most non-synergistic muscle pairs (colored in white), except the BRD-TRllong pair that showed significantly higher coherence strength in stroke patients than healthy participants at β and low γ bands ($p = 0.014$ and $p < 0.01$, respectively).

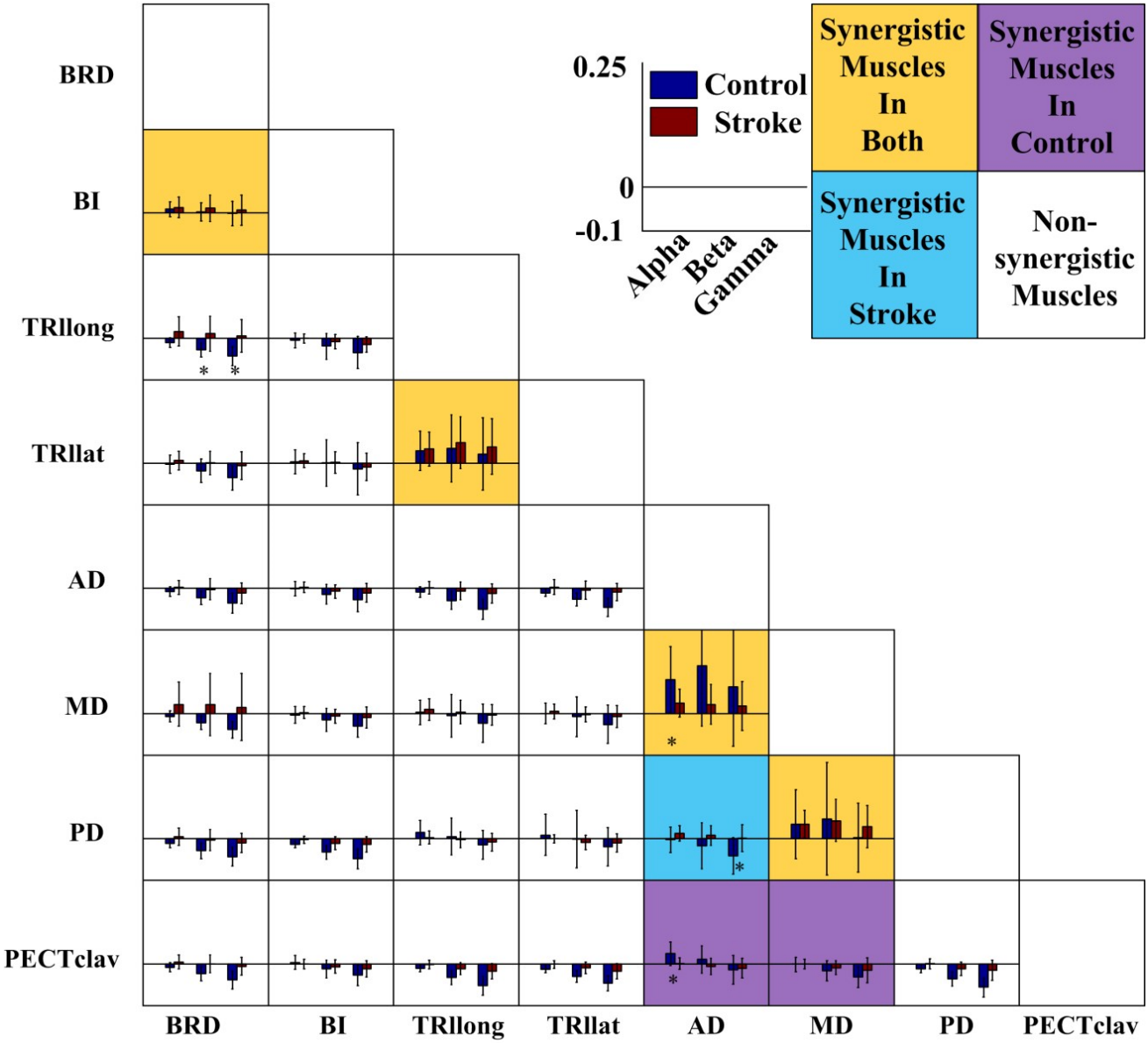

Figure 4. Statistical comparisons of IMC strength (assessed by the significant coherence area) of all muscle pairs between the control and stroke groups. The black horizontal line denotes the significant coherence area at confidence level. The "*" denotes a significant ($p < 0.05$) difference in the significant coherence area between two groups at each frequency band.

3.3. The combination of inter-muscular coherence and traditional evaluation scale

In order to appraise stroke patients' motor function from the perspective of neural control and provide effective guidance for rehabilitation, combined with the traditional Fugl-Meyer scale [33], the significant coherence area of synergistic muscle pairs are chosen to be an auxiliary index for evaluation.

With the help of the information of intermuscular synergy and intermuscular coherence, the traditional scale evaluation method can analyze the impact of stroke more specifically.

To inspect the relationship between the coherence of synergistic muscle pairs and the score of traditional Fugl-Meyer scale, Pearson correlation analysis was performed between patient's significant coherence area in α, β and γ bands and the patient's Fugl-Meyer score. The results are shown in the Figure 5. It can be seen that there was a prominent positive correlation between the significant coherence area in α, β and γ bands and the Fugl-Meyer score. The correlation coefficient R in α, β and γ bands were 0.7941, 0.7096 and 0.7569, respectively, and there was significant correlation ($p < 0.05$) in the three frequency bands. With the recovery of motor function, Fugl-Meyer score gradually increased and the coherence between synergistic muscle pairs also increased. These results show that the coherence of synergistic muscle pairs can be used to evaluate stroke patients' motor function. In addition, for specific muscle pairs, the difference of coherence can be discovered, which can provide targeted theoretical basis for rehabilitation.

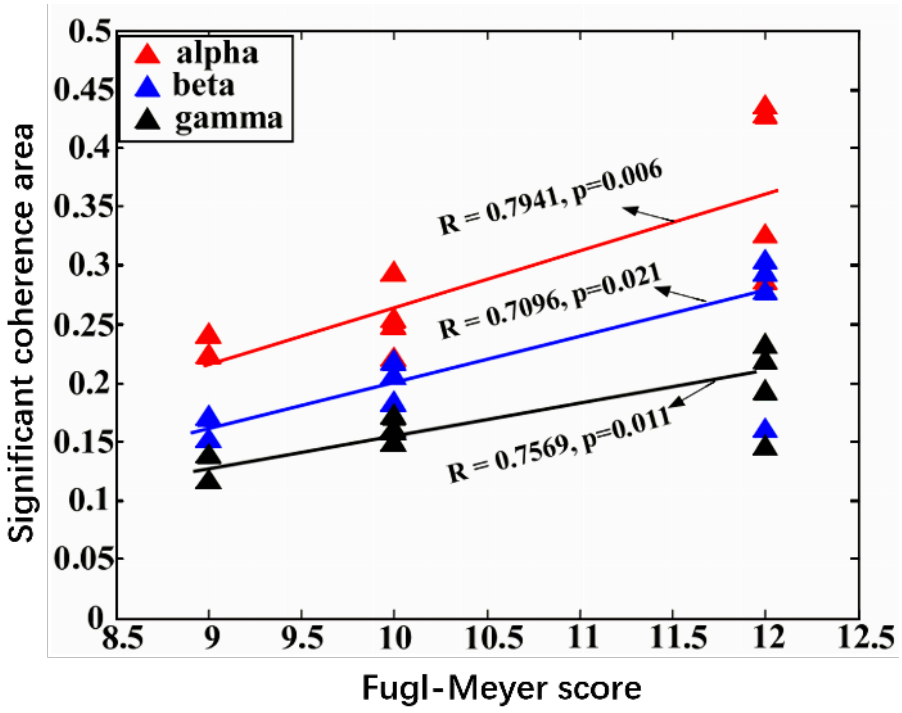

Figure 5. Correlation analysis between significant coherence area in α, β and γ bands and Fugl-Meyer score in stroke patients.

4. Discussion

The major contribution of this study is to ascertain how stroke alters the coherence strength of synergistic and non-synergistic muscle pairs during isometric force generation in the human upper limbs. As can be seen from our results, stroke not only causes abnormal coordination of muscle activation [9] but also alters the IMC between synergistic and non-synergistic muscle pairs in the human arm. In particular, our results demonstrate that IMC is able to expand the findings of muscle

synergy analysis by assessing the neural synchronization strength between any possible muscle pairs whose activation was recorded during motor tasks, which may give a potential mechanism for the formation of abnormal intermuscular coordination after stroke and hold great potential for the precise quantification of motor function recovery after stroke.

4.1. Muscle synergy and inter-muscular coherence

Neural synchronization has been considered as a mechanism that integrates the distributed sensory and motor systems involved in coordinating complex motion. Bernstein previously conceived the idea of modularity in motor coordination and hypothesized that the CNS would be able to co-activate a group of muscles to overcome the issue of "many degrees-of-freedom" in motor control [7]. d'Avella further defined muscle synergies by utilizing computational algorithms and proposed that muscle synergies consisted of the activation weights of a group of skeletal muscles and was coordinated by descending correlated neural commands [13]. Recent studies, from the perspective of neuronal oscillations that convey motor control information, suggested IMC would be able to reflect the correlated neural inputs between muscles in healthy control [19, 20, 22]. With this in mind, by incorporating the muscle synergy and coherence analysis, in this study we attempted to conduct a comprehensive study to investigate the relation between muscle coordination and IMC on healthy subjects and stroke patients.

As demonstrated in Figure 2, all synergistic muscle pairs in the control group (BRD-BI, TRIlat-TRIlong, AD-MD, MD-PD, AD-PECTclav and MD-PECTclav) showed higher coherence than the confidence level at all task sub-spaces, while the non-synergistic muscle pairs in the same group, such as AD-PD and PD-PECTclav, were mostly below confidence level. A similar tendency was also observed in our stroke group (Figure 3).

As can be seen from Table 3, in each subspace, there was a significant difference in the coherence strength between synergistic and non-synergistic muscle pairs. The results of statistical analysis further proved our conclusion. In general, muscle synergy represents the anatomical coordination of muscle activation in time when performing a specific motor task. It means that the oscillatory coupling and synchronous discharge of neurons play an important role in the process of human motion control. And muscle synergy is considered to be the minimum control mode of nerve center controlling movement [13]. It gives rise to a hypothesis that a synergistic muscle pair might be modulated by correlated neural input from CNS. Previous studies have partly addressed this hypothesis by showing that IMC is significantly higher in synergistic muscle pairs in healthy subjects [34, 35]. In this study, we have fully corroborated this finding and further expanded the existing knowledge by investigating the coherence of synergistic or non-synergistic muscle pairs in stroke with severe impairment. More specifically, the correlated neural input, defined by IMC, was significantly higher between synergistic muscle pairs that are anatomically closely related (defined by muscle synergy) in both healthy and stroke participants, respectively (Figures 2 and 3, Table 1). This consistent relationship between IMC and muscle synergy analyses could provide a new perspective to understand the possible neural mechanisms underlying the coordination of synergistic muscles in motor control.

4.2. The assessment of motor function by inter-muscular coherence

Beyond the significantly higher coherence in synergistic muscles shown in both control and stroke groups, respectively, emerging evidence has demonstrated that motor impairment could lead to the alteration of IMC strength over a wide frequency range in stroke patients. For instance, EMG oscillation within 6 to 12 Hz is considered evidence of a slow motion control mechanism [36], while motor unit synchronization in the β (15–30 Hz) and low γ (30–60 Hz) bands was mainly driven by the primary motor cortex and was less affected by the premotor cortices and supplementary motor [37–39]. In stroke patients, Farmer and Norton found that the muscular coupling was significantly suppressed in β band after stroke [40, 41]. These studies, however, lacked an anatomical criterion to localize the co-activated muscles for a rigorous analysis. It indicated that it was difficult for them to accurately locate the muscle pairs related to the injury. Or can only the muscles be analyzed as a whole rather than as a part. Therefore, it was difficult to justify the results in a physiologically-related manner. In the current study, taking advantage of muscle synergy, we were able to precisely target the potential muscle pairs that were closely associated with stroke-linked motor impairment.

Overall, we found significant alterations of IMC in several synergistic muscle pairs in stroke. More specifically, in the stroke group, the AD-MD pair revealed significantly lower IMC at α band compared to the control group, whereas significantly higher IMC between AD-PD at low γ band was observed in the patient group (Figure 4). Importantly, among the four synergistic muscle pairs identified in both groups, except for AD-MD muscles, no significant impaired coupling in patients was observed. Considering that IMC between muscles may represent a common neural input from CNS and oscillation within α band is considered to indicate pulsatile communication between the brain and muscle [42], the decrease in the coherence strength of AD-MD muscle pair could be a reflection of CNS' inability to sufficiently co-activate the target muscle. As such, the significantly higher IMC between AD-PD muscles in stroke patients, which was identified as a stroke-only synergistic muscle pair, might serve as a compensatory neuro-pathway for the insufficient corticospinal input generated from the CNS to control the AD-MD muscles. Additionally, the IMC between PECT-AD muscle pair, which was identified as synergistic muscle pair only in the healthy group, was significantly higher at α band in healthy controls as compared to stroke patients (Figure 4). This finding again supports the hypothesis that the coordinated pattern of synergistic muscles in stroke patients might be altered due to the loss or reduced correlated neural inputs from the CNS.

Our results show that motor units usually operate at a frequency of 5 to 12 Hz [43], which indicates that there is a correlation between the oscillation generated in the center and the ignition rate of the motor unit. During the stroke, the ignition rate and emission fluctuations of the motor unit will change. Among them, AD-MD, AD-PECTclav, in the α segment, were significantly reduced in stroke. Most studies examining cortical muscle coherence showed that low-frequency oscillations of neuromuscular signals are of a central origin (inferior olive, thalamocortical loop, motor cortex [2]). Abnormalities in cortical control are responsible for the loss of α fragments in stroke patients. The existence of coherence between low γ muscles can be explained by the need to quickly integrate information under dynamic conditions and generate appropriate movement commands, so it may reflect cortical-muscle coupling in the same frequency band between cortical activity and individual muscles. AD-PD is a synergistic muscle pair only in stroke patients, and its coherence significantly increased in stroke. The result may imply the high integration of AD-PD, which leads to the movement of stroke patients being

constrained.

Apart from the structural localization provided by muscle synergy analysis, the IMC holds great potential in assessing the strength of neural synchronization between a pair of muscle that couldn't be captured by muscle synergy analysis. Specifically, in our study four synergistic muscle pairs were identified in both healthy and patient groups based on muscle synergy analysis, wherein one synergistic muscle pair (AD-MD) was found to have significantly low IMC in the patient group. This finding suggests that, while the structural coordination of movement control obtained by muscle synergy analysis seems to be consistent in healthy controls and stroke patients, the strength of neural synchronization driven by the CNS may have been partially affected by stroke in particular muscle pair. In addition, although the BRD-TRI muscle pair was identified as non-synergistic muscles in both groups, there was abnormally high neural synchronization between these two muscles in stroke patients as indicated by the IMC result (Figure 4), which supports that IMC is capable of detecting impaired neural pathways after stroke that could not be captured by muscle synergy. Taking these together, the integrated analysis of muscle synergies and IMC is not only able to spatiotemporally identify typical co-activation patterns of muscles but also functionally quantify the strength of neural synchronization among these muscles, allowing more comprehensive investigation of the neural mechanism underlies motor function recovery and motor control after stroke.

4.3. Limitations

In this study, to obtain a robust set of EMG signals activated during isometric force generation tasks from stroke patients, each of the 54 force target matches was repeated only once, which limited the amount of EMG data for the calculation of coherence. To overcome the small trial number, we concatenated the EMG data of force target matches if the target directions were classified within the same sub-space. However, it would be ideal to have enough repeats per each target force direction so that the data concatenation would not be required. Additionally, in this preliminary study, only 10 patients were recruited to participate in the experiment. It is expected that the result obtained in the present study could be validated on a larger cohort in a future study. In this study, only the coherence of the synergistic and non-synergistic muscles was compared, while the degree of activation in all space was not discussed, so it should be considered to include the activation coefficient in further research and analysis. Our statistical tests showed that the synergistic muscle pair (AD-MD) revealed significantly lower IMC in the patient group, though four synergistic muscle pairs were found in both the patient and control groups (Figure 4). Results also showed there is no significant difference between TRllong-TRllat. Taken together, we hypothesized that the reduction of coherence between AD-MD may reflect the change of CNS control strategy after stroke.

5. Conclusions

In this study, we analyzed the inter-muscular coherence and muscle coordination based on the EMG signals recorded during a 3-D isometric force task involved healthy and stroke participants, respectively. The outcome of a traditional NMF-based muscle synergy analysis highlighted a modular organization of motor coordination when performing a target task. Furthermore, the intermuscular coherence analysis demonstrated a significantly higher coherence in the pairs of synergistic muscles compared to those of non-synergistic muscles in both healthy and patient groups, respectively,

meaning that spatiotemporally correlated muscle pairs would receive synchronized neural inputs. In addition, the coherence strengths of several synergistic muscle pairs were found to be significantly altered in stroke patients. This study could contribute to the investigation of the mechanism of motor control and provides a promising approach to assess the motor function recovery in stroke patients.

Acknowledgments

This work was supported by the National Nature Science Foundation of China (Grant No.61971168, 61871427), Zhejiang Provincial Key R&D Program of China (No.2021C03031), the Open Research Projects of Zhejiang Lab (No. 2021MC0AB04)

Conflict of interest

All authors declare no conflicts of interest in this paper.

References

1. V. L. Feigin, B. A. Stark, C. O. Johnson, G. A. Roth, C. Bisignano, G. Abady, et al., Global, regional, and national burden of stroke and its risk factors, 1990–2019: a systematic analysis for the Global Burden of Disease Study 2019, *Lancet Neurol.*, **20** (2020), 795–820. https://doi.org/10.1016/S1474-4422(21)00252-0
2. K. Kisiel-Sajewicz, Y. Fang, K. Hrovat, G. H. Yue, V. Siemionow, C. Sun, et al., Weakening of synergist muscle coupling during reaching movement in stroke patients, *Neurorehabil. Neural Repair*, **25** (2011), 359–368. https://doi.org/10.1177/1545968310388665
3. R. F. Beer, J. D. Given, J. P. Dewald, Task-dependent weakness at the elbow in patients with hemiparesis, *Arch. Phys. Med. Rehabil.*, **80** (1999), 766–772. https://doi.org/10.1016/S0003-9993(99)90225-3
4. Y. Lan, J. Yao, J. P. Dewald, The impact of shoulder abduction loading on volitional hand opening and grasping in chronic hemiparetic stroke, *Neurorehabil. Neural Repair*, **31** (2017), 521–529. https://doi.org/10.1177/1545968317697033
5. T. M. Sukal, M. D. Ellis, J. P. Dewald, Shoulder abduction-induced reductions in reaching work area following hemiparetic stroke: neuroscientific implications, *Exp. Brain Res.*, **183** (2007), 215–223. https://doi.org/10.1007/s00221-007-1029-6
6. P. H. McCrea, J. J. Eng, A. J. Hodgson, Saturated muscle activation contributes to compensatory reaching strategies after stroke, *J. Neurophysiol.*, **94** (2005), 2999–3008. https://doi.org/10.1152/jn.00732.2004
7. N. Bernstein, *The co-ordination and regulation of movements*, Pergamon Press, 1966.
8. M. M. DaSilva, V. D. Chandran, P. C. Dixon, J. M. Loh, J. T. Dennerlein, J. M. Schiffman, et al., Muscle co-contractions are greater in older adults during walking at self-selected speeds over uneven compared to even surfaces, *J. Biomech.*, **128** (2021). https://doi.org/10.1016/j.jbiomech.2021.110718

9. J. Roh, W. Z. Rymer, E. J. Perreault, S. B. Yoo, R. F. Beer, Alterations in upper limb muscle synergy structure in chronic stroke survivors, *J. Neurophysiol.*, **109** (2013), 768–781. https://doi.org/10.1152/jn.00670.2012
10. J. Roh, W. Z. Rymer, R. F. Beer, Evidence for altered upper extremity muscle synergies in chronic stroke survivors with mild and moderate impairment, *Front. Hum. Neurosci.*, **9** (2015), 6. https://doi.org/10.3389/fnhum.2015.00006
11. D. J. Clark, L. H. Ting, F. E. Zajac, R. R. Neptune, S. A. Kautz, Merging of healthy motor modules predicts reduced locomotor performance and muscle coordination complexity post-stroke, *J. Neurophysiol.*, **103** (2009), 844–857. https://doi.org/10.1152/jn.00670.2012
12. M. Goudriaan, E. Papageorgiou, B. R. Shuman, K. M. Steele, N. Dominici, A. Van Campenhout, et al., Muscle synergy structure and gait patterns in children with spastic cerebral palsy, *Dev. Med. Child Neurol.*, (2021). https://doi.org/10.1111/dmcn.15068
13. A. d'Avella, P. Saltiel, E. Bizzi, Combinations of muscle synergies in the construction of a natural motor behavior, *Nat. Neurosci.*, **6** (2003), 300. https://doi.org/10.1038/nn1010
14. X. Li, Y. Du, C. Yang, W. Qi, P. Xie, Merging of synergistic muscles and intermuscular coherence predict muscle coordination complexity, in *2016 IEEE International Conference on Information and Automation (ICIA)*, (2016), 791–795. https://doi.org/10.1109/ICInfA.2016.7831927
15. Y. Gao, X. Wang, T. Potter, J. Zhang, Y. Zhang, Single-trial EEG emotion recognition using Granger Causality/Transfer Entropy analysis, *J. Neurosci. Methods.*, **346** (2020), 108904. https://doi.org/10.1016/j.jneumeth.2020.108904
16. Y. Gao, L. Ren, R. Li, Y. Zhang, Electroencephalogram–Electromyography Coupling Analysis in Stroke Based on Symbolic Transfer Entropy, *Front. Neurol.*, **8** (2018). https://doi.org/10.3389/fneur.2017.00716
17. Y. Liu, X. Xu, Y. Zhou, J. Xu, X. Dong, X. Li, et al., Coupling feature extraction method of resting state EEG Signals from amnestic mild cognitive impairment with type 2 diabetes mellitus based on weight permutation conditional mutual information, *Cogn. Neurodyn.*, (2021), 1–11. https://doi.org/10.1007/s11571-021-09682-1
18. C. De Marchis, A. M. Castronovo, D. Bibbo, M. Schmid, S. Conforto, Muscle synergies are consistent when pedaling under different biomechanical demands, in *2012 Annual International Conference of the IEEE Engineering in Medicine and Biology Society*, (2012), 791–795. https://doi.org/10.1109/EMBC.2012.6346672
19. K. M. Fisher, B. Zaaimi, T. L. Williams, S. N. Baker, M. R. Baker, Beta-band intermuscular coherence: a novel biomarker of upper motor neuron dysfunction in motor neuron disease, *Brain*, **135** (2012), 2849-2864. https://doi.org/10.1093/brain/aws150
20. G. Hu, W. Yang, X. Chen, W. Qi, X. Li, Y. Du, et al., Estimation of time-varying coherence amongst synergistic muscles during wrist movements, *Front. Neurosci.*, **12** (2018). https://doi.org/10.3389/fnins.2018.00537
21. S. Farmer, Rhythmicity, synchronization and binding in human and primate motor systems, *J. Physiol.*, **509** (1998), 3–14. https://doi.org/10.1111/j.1469-7793.1998.003bo.x

22. C. De Marchis, G. Severini, A. M. Castronovo, M. Schmid, S. Conforto, Intermuscular coherence contributions in synergistic muscles during pedaling, *Exp. Brain Res.*, **233** (2015), 1907–1919. https://doi.org/10.1007/s00221-015-4262-4

23. D. Mayhew, B. Bachrach, W. Z. Rymer, R. F. Beer, Development of the MACARM - a novel cable robot for upper limb neurorehabilitation, in *2016 International Conference on Rehabilitation Robotics*, 2016. https://doi.org/10.1109/ICORR.2005.1501106

24. R. F. Beer, C. Naujokas, B. Bachrach, D. Mayhew, Development and evaluation of a gravity compensated training environment for robotic rehabilitation of post-stroke reaching, in *2008 IEEE Ras & Embs International Conference on Biomedical Robotics & Biomechatronics*, 2008. https://doi.org/10.1109/BIOROB.2008.4762863

25. D. D. Lee, H. S. Seung, Learning the parts of objects by non-negative matrix factorization, *Nature*, **401** (1999), 788. https://doi.org/10.1038/44565

26. L. H. Ting, J. M. Macpherson, A limited set of muscle synergies for force control during a postural task, *J. Neurophysiol.*, **93** (2005), 609–613. https://doi.org/10.1152/jn.00681.2004

27. M. C. Tresch, V. C. K. Cheung, A. d'Avella, Matrix factorization algorithms for the identification of muscle synergies: evaluation on simulated and experimental data sets, *J. Neurophysiol.*, **95** (2006), 2199–2212. https://doi.org/10.1152/jn.00222.2005

28. L. J. Myers, M. Lowery, M. O'Malley, C. L. Vaughan, C. Heneghan, A. Gibson, et al., Rectification and non-linear pre-processing of EMG signals for cortico-muscular analysis, *J. Neurosci. Methods.*, **124** (2003), 157–165. https://doi.org/10.1016/S0165-0270(03)00004-9

29. S. F. Farmer, J. Gibbs, D. M. Halliday, L. M. Harrison, L. M. James, M. J. Mayston, et al., Changes in EMG coherence between long and short thumb abductor muscles during human development, *J. Physiol.*, **579** (2007), 389–402. https://doi.org/10.1113/jphysiol.2006.123174

30. R. Fisher, M. Galea, P. Brown, R. Lemon, Digital nerve anaesthesia decreases EMG-EMG coherence in a human precision grip task, *Exp. Brain Res.*, **145** (2002), 207–214. https://doi.org/10.1007/s00221-002-1113-x

31. C. M. Laine, F. J. Valero-Cuevas, Intermuscular coherence reflects functional coordination, *J. Neurophysiol.*, **118** (2017), 1775–1783. https://doi.org/10.1152/jn.00204.2017

32. J. Roh, S. Lee, K. D. Wilger, Modular organization of exploratory force development under isometric conditions in the human arm, *J. Mot. Behav.*, **51** (2019), 83–99. https://doi.org/10.1080/00222895.2017.1423020

33. D. J. Gladstone, C. J. Danells, S. E. Black, The Fugl-Meyer assessment of motor recovery after stroke: a critical review of its measurement properties, *Neurorehabil. Neural. Repair*, **16** (2002), 232–240. https://doi.org/doi: 10.1177/154596802401105171

34. A. Danna-Dos-Santos, T. W. Boonstra, A. M. Degani, V. S. Cardoso, A. T. Magalhaes, L. Mochizuki, et al., Multi-muscle control during bipedal stance: an EMG–EMG analysis approach, *Exp. Brain Res.*, **232** (2014), 75–87. https://doi.org/10.1007/s00221-013-3721-z

35. A. Danna-Dos-Santos, A. M. Degani, T. W. Boonstra, L. Mochizuki, A. M. Harney, M. M. Schmeckpeper, et al., The influence of visual information on multi-muscle control during quiet stance: a spectral analysis approach, *Exp. Brain Res.*, **233** (2015), 657–669. https://doi.org/10.1007/s00221-014-4145-0

36. A. Vallbo, J. Wessberg, Organization of motor output in slow finger movements in man, *J. Physiol.*, **469** (1993), 673–691. https://doi.org/10.1113/jphysiol.1993.sp019837

37. J. F. Marsden, P. Brown, S. Salenius, Involvement of the sensorimotor cortex in physiological force and action tremor, *Neuroreport*, **12** (2001), 1937–1941. https://doi.org/10.1097/00001756-200107030-00033

38. Y. Chen, S. Li, E. Magat, P. Zhou, S. Li, Motor Overflow and Spasticity in Chronic Stroke Share a Common Pathophysiological Process: Analysis of Within-Limb and Between-Limb EMG-EMG Coherence, *Front. Neurol.*, (2018). https://doi.org/10.3389/fneur.2018.00795

39. H. Obata, M. O. Abe, K. Masani, K. Nakazawa, Modulation between bilateral legs and within unilateral muscle synergists of postural muscle activity changes with development and aging, *Exp. Brain Res.*, **232** (2013), 1–11. https://doi.org/10.1007/s00221-013-3702-2

40. S. Farmer, M. Swash, D. Ingram, J. Stephens, Changes in motor unit synchronization following central nervous lesions in man, *J. Physiol.*, **463** (1993), 83–105. https://doi.org/10.1113/jphysiol.1993.sp019585

41. J. A. Norton, D. E. Wood, J. F. Marsden, B. L. Day, Spinally generated electromyographic oscillations and spasms in a low-thoracic complete paraplegic, *Mov. Disord.*, **18** (2003), 101–106. https://doi.org/10.1002/mds.10298

42. E. Lattari, B. Velasques, F. Paes, M. Cunha, H. Budde, L. Basile, Corticomuscular coherence behavior in fine motor control of force: a critical review, *Rev. Neurol.*, **51** (2010), 610. https://doi.org/10.33588/rn.5110.2010311

43. R. S. Person, L. P. Kudina, Discharge frequency and discharge pattern of human motor units during voluntary contraction of muscles, *Electroencephalogr. Clin. Neurophysiol.*, **32** (1972), 471–483. https://doi.org/10.1016/0013-4694(72)90058-2

AIMS Press